JCTC Journal of Chemical Theory and Computation

DFT Calculations of Isotropic Hyperfine Coupling Constants of Nitrogen Aromatic Radicals: The Challenge of Nitroxide Radicals

L. Hermosilla, J. M. García de la Vega, C. Sieiro, and P. Calle*

Departamento de Química Física Aplicada, Facultad de Ciencias, Universidad Autónoma de Madrid, 28049 Madrid, Spain

Received October 26, 2010

Abstract: The performance of DFT methodology to predict with accuracy the isotropic hyperfine coupling constants (hfccs) of aromatic radicals containing ^{14}N nucleus is investigated by an extensive study in which 165 hfccs, belonging to 38 radical species, are obtained from calculations with B3LYP and PBE0 functionals combined with 6-31G*, N07D, TZVP, and EPR-III basis sets, and are compared to the reported experimental data. The results indicate that the selection of the basis set is of fundamental importance in the calculation of ^{14}N hfccs, whereas there is not so great an influence on the accurate computation of that parameter for ^{1}H nuclei. The values of the calculated ^{14}N coupling constants of aromatic nitroxide radicals using DFT methodology are noticeably lower than the experimental ones. A very simple relation to predict these hfccs with high accuracy is proposed on the basis of the present results, as an interesting alternative to the highly computationally demanding integrated approaches so far used.

I. Introduction

Free radicals containing nitrogen nucleus are present in many processes of chemical, physical, and biological interest. Thus, the knowledge of their electronic distribution is very valuable to get an insight into those processes. Especially remarkable is the interest in nitroxide radical chemistry, due to their role as spin labels and spin probes, thanks to their characteristic long lives and spectromagnetic properties.[1] The nuclear hyperfine interaction, experimentally measured by electron paramagnetic resonance (EPR) spectroscopy, provides information about the electronic distribution, so the correct interpretation of the EPR spectra is of fundamental importance.[2,3] In this regard, quantum mechanical (QM) calculations can act as an effective tool for that challenge.[4] The interaction between magnetic nuclei and unpaired electrons is represented by the hyperfine tensor, which can be factored into both an isotropic (spherically symmetric) and an anisotropic (dipolar) term. The isotropic term (a_{iso}), so-called isotropic hyperfine coupling constant (hfcc), depends on the spin density at the nucleus position, making this property very sensitive to the level of the calculation, specifically to the electron correlation, the one-electron basis set, and the use of an adequate molecular geometry.

In previous papers,[5−8] we investigated the reliability of density functional theory (DFT) methodology to compute hfccs of different nuclei of a large number of both organic and inorganic radicals on their ground state. The main conclusion was that the best overall results are obtained when B3LYP[9,10] functional is combined with TZVP[11] or EPR-III[12,13] basis sets, yielding highly accurate values of hfccs of nuclei belonging to the three first rows. An exception was found for the ^{14}N nuclei in which the smaller and less computationally demanding 6-31G*[14,15] basis set yields hfcc values closer to the experimental ones, probably due to the fact that it has six *d* functions instead of the five *d* functions of the TZVP and EPR-III basis sets, providing an additional *s* function to complete the *s* space.

Afterward, Barone and co-workers developed a new polarized split-valence basis set for the calculation of hfccs of second- and third-row atoms, the so-called N07D,[16,17] by adding a reduced number of polarization and diffuse functions to the 6-31G set. In order to get accurate values of the hfccs and retain, or even improve, the good performance of the parent 6-31G* basis set for other properties dominated

* Corresponding author e-mail: paloma.calle@uam.es.

10.1021/ct1006136
Published on Web 12/02/2010

by valence orbitals, the new set was tailored by optimizing the core−valence *s* functions and reoptimizing polarization and diffuse *p* functions. Such a parametrization was made specifically for both the B3LYP and the parameter free PBE0[18] functionals. These authors reported calculations on a large set of radicals, in which the results obtained with B3LYP/N07D and PBE0/N07D combinations were compared to those produced by 6-31G*, TZVP and EPR-III basis sets, all in conjunction with B3LYP functional. The general conclusion was that both computational models, B3LYP/N07D and PBE0/N07D, provide good agreement with experimental data and predictive power at lower computational cost. For radicals containing oxygen and nitrogen atoms, they obtained poorer correlation between computations and experiments.[16] These lower correlation coefficients for ^{14}N and ^{17}O could be related to the reduced range of experimental data (about 30 G).

As far as we know, all previous works performed on large sets of radicals with the aim of establishing a computational protocol able to predict $a_{iso}(^{14}N)$ with high reliability, are mainly performed on nonaromatic nitrogen radicals, even though the aromatic counterparts have a lot of applications in different fields, specially nitroxide radicals, that are probably the most widely used spin probes and spin labels. The lack of a systematic theoretical study on hfccs of aromatic nitrogen radicals, which is expected to arouse a lot of interest, prompted us to investigate the performance of DFT methodology to predict with precision such constants in this work. The main goal is undertaken by performing an extensive study on a set of conjugated radicals containing ^{14}N nucleus, in which calculation of the hfccs is carried out with the levels of theory formerly proved as the most adequate for the evaluation of this constant, that is, by employing B3LYP and PBE0 functionals combined with 6-31G*, N07D, TZVP and EPR-III basis sets on the previously optimized structures. Computed values are compared to the available experimental data by a statistical analysis. Besides the conclusions regarding the accuracy of the different methodologies on the prediction of this magnetic property, this work seeks to be a useful tool for EPR spectroscopists, since it facilitates the correct assignment of the experimental hfccs from reliable theoretical values.

II. Computational Details

A set of 38 neutral aromatic radicals containing at least one ^{14}N nucleus (nuclear spin $I = 1$) is considered in this study. Their schematic structures are depicted in Figure 1. The molecular geometries of the radicals on their electronic ground state are fully optimized at the B3LYP level employing the 6-31G* basis set due to its low computational cost and good results according to previous works.[5−8] Harmonic vibrational frequencies are computed at the same level of theory as the geometry optimization to confirm the nature of the stationary points. The hfccs of the radicals are evaluated on the optimized structures at five different levels of theory: PBE0/N07D, B3LYP/6-31G*, B3LYP/N07D, B3LYP/TZVP, and B3LYP/EPR-III.

The 6-31G* basis set is a small double-ζ basis plus polarization, whereas the TZVP is a DFT-optimized valence triple-ζ basis. EPR-III is a larger basis set (triple-ζ basis including diffuse functions, double *d*-polarizations, and a single set of *f*-polarization functions) optimized for the computation of hfccs by DFT methods. As previously mentioned, N07D is a polarized split-valence basis set also developed for the calculation of hfccs with an optimum compromise between reliability and computer time.[16,17] It is important to note that, although it has the same name, N07D basis set is slightly different for application with either the B3LYP or the PBE0 functional, since it has been parametrized specifically for each of them. The standard programs for the calculation of molecular structures use five *d* Cartesian Gaussian functions for TZVP and EPR-III basis sets, and six *d* functions for 6-31G* basis set. The redundant set of six *d* functions has to be employed also for N07D basis set, since it has been developed with this feature.[16,17] All calculations are carried out with the Gaussian03 software package.[19]

III. Results and Discussion

A total of 165 hfccs for the radicals drawn in Figure 1 has been calculated, on the corresponding optimized geometries, those with available experimental data, from which 47 are a_{iso} of ^{14}N and 114 are a_{iso} of ^{1}H. The four remaining coupling constants, which correspond to ^{33}S, ^{13}C, and ^{17}O nuclei, have not been taken into account in the data analysis, being the target of the paper comparison between calculated and experimental hfccs of ^{14}N and ^{1}H nuclei.

The name, the symmetry of the electronic ground state, and the total energies corresponding to the minimum for each radical, computed at the five different levels of theory, are shown in Table S1 in the Supporting Information (SI).

The calculated and the experimental a_{iso} are summarized in Table 1. The first column corresponds to the number of each radical. The second column indicates the nuclei with their mass numbers, preceded by a number to indicate the equivalent atoms, and with a subscript to identify the nonequivalent atoms unequivocally, when necessary. The following five columns report the theoretical hfcc values obtained at the different levels of theory. In the last two columns, the experimental hfccs and their bibliographic references are given. As is well-known, the sign of a_{iso} is not determined by EPR experiments; it is assigned on the basis of theoretical results. Thus, the experimental data are given as absolute values and the sign has been included just in the theoretical data. The assignment of the specified pairs of experimental hfccs of radicals **8**, **13**, and **34** has been exchanged according to the theoretical results obtained in this work.

A general inspection of the data shown in Table 1 indicates that the a_{iso} of ^{1}H are predicted in very good agreement with the experimental values, regardless of the level of theory employed. However, different conclusions are extracted from the observation of the theoretical values of $a_{iso}(^{14}N)$. In general, 6-31G* and N07D basis set present the best predictive behavior, yielding values closer to the experimental data than those obtained by EPR-III or TZVP basis sets, which tend to underestimate $a_{iso}(^{14}N)$, specially TZVP

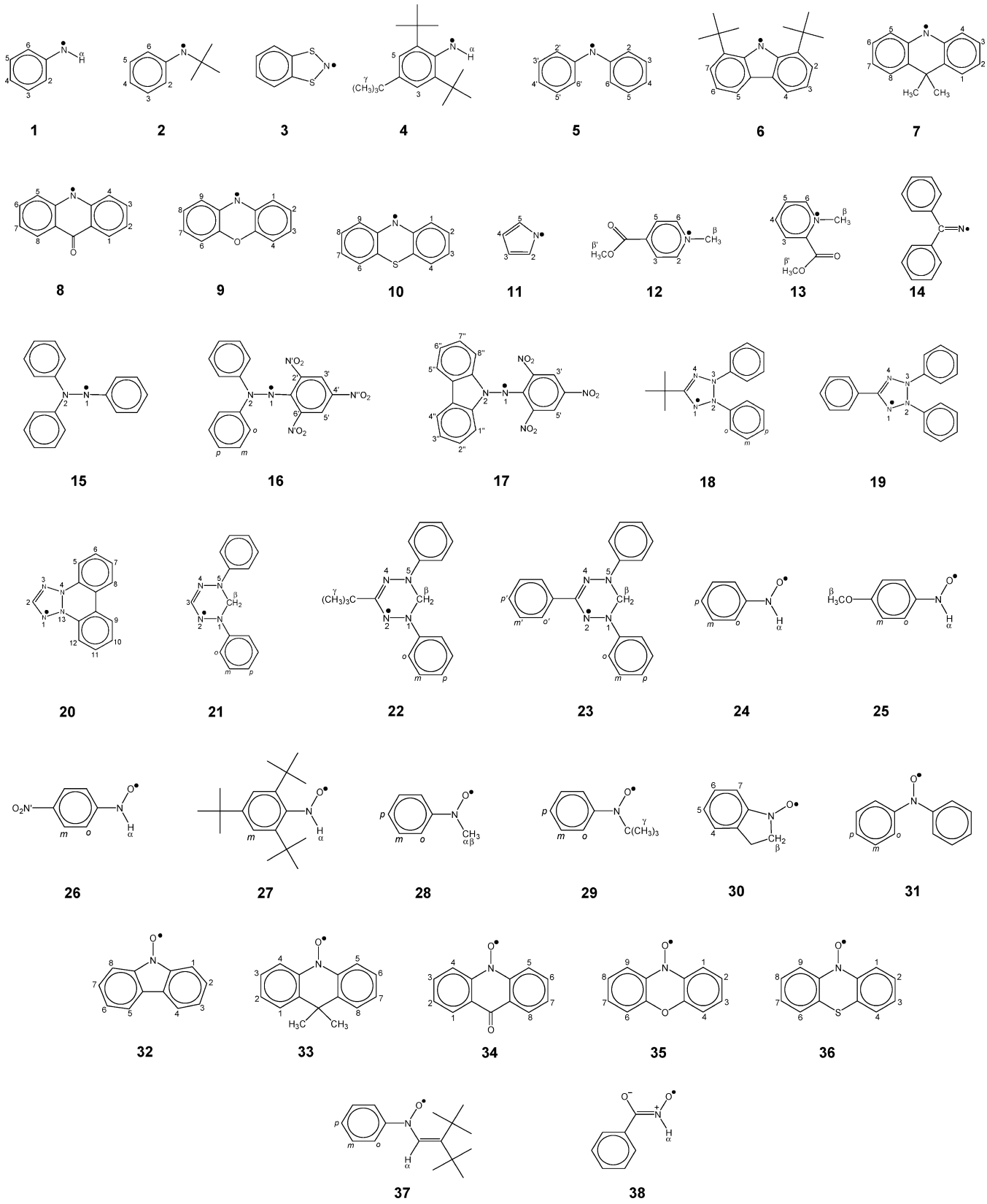

Figure 1. Geometrical structures of the studied radicals.

basis set. These results are consistent with that obtained in our previous work on nitrogen coupling constants of non-aromatic radicals,[8] which pointed out that the 6-31G* basis set leads to more accurate results than TZVP and EPR-III basis sets, in spite of being smaller. The additional *s* function implicitly added when using a 6 *d* set plays a non negligible role in completing the *s* space, and thus in obtaining more accurate hfccs, in case of small or medium size basis sets (e.g., 6-31G*, N07D). However, this is not the case for larger basis sets like TZVP and EPR-III, since the results are very similar using either 5 or 6 *d* functions.[8,16,17] Accordingly, a set of 5 *d* functions is the standard for TZVP and EPR-III

Table 1. Theoretical Isotropic Hyperfine Coupling Constants (G) of the Studied Radicals Calculated at Different Levels of Theory[a]

no.	nuclei	a_{iso} (theoretical)					experimental	
		PBE0/N07D	B3LYP/6-31G*	B3LYP/N07D	B3LYP/TZVP	B3LYP/EPR-III	a_{iso}	ref
1	^{14}N	+9.6	+9.3	+9.2	+6.1	+7.3	7.95	20
	$^{1}H_{\alpha}$	−14.0	−14.7	−14.5	−14.1	−13.8	12.94	
	$^{1}H_{2,6}$	−6.7	−6.8	−6.7	−6.2	−6.3	6.18	
	$^{1}H_{3,5}$	+3.2	+2.9	+2.7	+2.6	+2.7	2.01	
	$^{1}H_{4}$	−7.7	−7.9	−7.8	−7.3	−7.6	8.22	
2	^{14}N	+11.3	+10.7	+10.7	+7.5	+8.6	9.70	21
	$^{1}H_{2,6}$	−6.3	−6.4	−6.2	−5.7	−5.9	5.84	
	$^{1}H_{3,5}$	+3.0	+2.7	+2.4	+2.3	+2.4	1.99	
	$^{1}H_{4}$	−7.1	−7.3	−7.1	−6.6	−6.9	7.09	
3	^{14}N	+12.4	+11.3	+11.8	+8.7	[b]	11.0	22
	$2^{33}S$	+2.6	+2.7	+3.0	+3.1	[b]	3.9	
	$4^{1}H$	−0.5	−0.6	−0.6	−0.6	[b]	0.6	
4	^{14}N	−8.4	+8.6	+8.1	+5.5	+6.4	6.70	23
	$^{1}H_{\alpha}$	−12.4	−13.0	−12.8	−12.4	−12.2	11.75	
	$^{1}H_{3,5}$	+3.1	+2.7	+2.7	+2.4	+2.5	1.89	
	$9^{1}H_{\gamma}$	+0.2	+0.3	+0.3	+0.3	+0.3	0.27	
5	^{14}N	+9.9	+9.3	+9.2	+6.5	+7.4	8.80	24
	$^{1}H_{2,2',6,6'}$	−4.3	−4.4	−4.2	−3.9	−4.0	3.68	
	$^{1}H_{3,3',5,5'}$	+2.3	+2.1	+2.0	+1.9	+2.0	1.52	
	$^{1}H_{4,4'}$	−4.8	−4.8	−4.8	−4.4	−4.6	4.28	
6	^{14}N	+8.6	+8.1	+8.0	+5.5	+6.3	6.97	25
	$^{1}H_{2,7}$	+1.6	+1.4	+1.3	+1.2	+1.3	0.89	
	$^{1}H_{3,6}$	−4.4	−4.4	−4.4	−4.0	−4.2	4.30	
	$^{1}H_{4,5}$	+1.2	+0.4	+0.4	+0.4	+0.1	0.14	
7	^{14}N	+9.2	+8.4	+8.6	+5.9	+6.8	8.00	24
	$^{1}H_{1,3,6,8}$	+2.2	+2.0	+1.9	+1.7	+1.8	1.28	
	$^{1}H_{2,7}$	−5.0	−5.0	−4.9	−4.6	−4.8	4.52	
	$^{1}H_{4,5}$	−4.4	−4.4	−4.3	−3.9	−4.1	3.67	
8	^{14}N	+8.0	+7.3	+7.4	+5.1	+5.9	6.98	24
	$^{1}H_{1,8}$	+1.6	+1.3	+1.2	+1.1	+1.1	0.76[c]	
	$^{1}H_{2,7}$	−4.5	−4.5	−4.4	−4.1	−4.3	4.12	
	$^{1}H_{3,6}$	+2.2	+1.9	+1.8	+1.6	+1.7	1.27[c]	
	$^{1}H_{4,5}$	−4.4	−4.3	−4.2	−3.9	−4.0	3.67	
9	^{14}N	+8.8	+8.1	+8.2	+5.7	+6.6	8.03	26
	$^{1}H_{1,9}$	−3.7	−3.7	−3.6	−3.3	−3.4	2.88	
	$^{1}H_{2,8}$	+1.5	+1.3	+1.2	+1.1	+1.1	0.97	
	$^{1}H_{3,7}$	−4.4	−4.4	−4.3	−4.0	−4.2	3.97	
	$^{1}H_{4,6}$	+1.6	+1.4	+1.3	+1.2	+1.3	0.65	
10	^{14}N	+8.1	+7.5	+7.5	+5.3	[b]	7.05	27
	$^{1}H_{1,9}$	−3.7	−3.7	−3.5	−3.2	[b]	2.85	
	$^{1}H_{2,4,6,8}$	+1.8	+1.5	+1.4	+1.3	[b]	0.95	
	$^{1}H_{3,7}$	−4.2	−4.3	−4.2	−3.9	[b]	3.66	
11	^{14}N	−3.2	−2.4	−2.6	−2.3	−2.4	2.91	28
	$^{1}H_{2,5}$	−13.5	−14.0	−13.8	−12.9	−13.4	13.26	
	$^{1}H_{3,4}$	−3.2	−3.4	−3.4	−3.2	−3.3	3.55	
12	^{14}N	+6.3	+5.8	+5.9	+4.5	+5.0	6.25	29
	$^{1}H_{2,6}$	−4.7	−5.1	−4.8	−4.5	−4.6	3.55	
	$^{1}H_{3,5}$	+0.4	+0.2	+0.1	+0.1	+0.1	0.8	
	$3^{1}H_{\beta}$	+5.2	+5.8	+5.1	+5.4	+5.7	5.55	
	$3^{1}H_{\beta'}$	+0.9	+0.9	+0.9	+0.9	+1.0	0.8	
13	^{14}N	+6.2	+5.6	+5.7	+4.3	+4.8	6.58	30
	$^{1}H_{3}$	+1.8	+1.6	+1.5	+1.4	+1.4	0.94	
	$^{1}H_{4}$	−6.7	−7.2	−6.9	−6.4	−6.6	6.28	
	$^{1}H_{5}$	−2.5	−2.8	−2.8	−2.6	−2.7	2.54[c]	
	$^{1}H_{6}$	−1.4	−1.6	−1.5	−1.3	−1.4	1.40[c]	
	$3^{1}H_{\beta}$	+5.8	+6.3	+6.0	+5.9	+6.4	5.64	
	$3^{1}H_{\beta'}$	+1.0	+0.5	+1.1	+1.1	+1.2	0.94	
14	^{14}N	+11.5	+11.0	+11.8	+6.7	+8.6	10	31
	$4^{1}H_{o},4^{1}H_{m}$	+0.3	+0.4	+0.4	+0.4	+0.4	0.37	
	$2^{1}H_{p}$	+0.2	+0.2	+0.2	+0.2	+0.2	<0.2	
15	$^{14}N_{1}$	+11.0	+10.7	+10.4	+7.8	+8.7	9.05	32
	$^{14}N_{2}$	+4.1	+4.1	+3.9	+2.6	+3.1	4.28	
16	$^{14}N_{1}$	+12.4	+12.1	+12.2	+10.5	+11.1	9.74	33
	$^{14}N_{2}$	+7.4	+7.0	+6.9	+5.1	+5.7	7.95	
	$2^{14}N'$	−0.4	−0.3	−0.3	−0.4	−0.3	0.39	34
	$^{14}N''$	−0.4	−0.3	−0.3	−0.4	−0.3	0.48	
	$^{1}H_{3',5'}$	+1.4	+1.2	+1.2	+1.2	+1.2	1.06	35
	$4^{1}H_{o}$	−1.8	−1.7	−1.7	−1.6	−1.6	1.55	
	$4^{1}H_{m}$	+1.0	+0.9	+0.9	+0.8	+0.9	0.73	
	$2^{1}H_{p}$	−1.7	−1.7	−1.7	−1.6	−1.7	1.58	
17	$^{14}N_{1}$	+14.0	+13.4	+13.6	+11.9	+12.4	11.1	36
	$^{14}N_{2}$	+5.3	+5.0	+5.0	+3.5	+4.1	6.0	
	$^{1}H_{3',5'}$	+1.5	+1.4	+1.4	+1.3	+1.4	1.17	
	$^{1}H_{1'',8''}$	−2.2	−2.2	−2.1	−2.0	−2.1	1.92	
	$^{1}H_{2'',7''}$	+0.8	+0.7	+0.7	+0.5	+0.7	0.53	
	$^{1}H_{3'',6''}$	−2.0	−2.1	−2.0	−1.9	−2.0	1.81	
	$^{1}H_{4'',5''}$	+0.7	+0.6	+0.5	+0.7	+0.5	0.41	

Table 1. Continued

no.	nuclei	a_{iso} (theoretical) PBE0/N07D	B3LYP/6-31G*	B3LYP/N07D	B3LYP/TZVP	B3LYP/EPR-III	experimental a_{iso}	ref
18	$^{14}N_{1,4}$	+6.5	+6.2	+6.1	+4.6	+5.1	5.7	37
	$^{14}N_{2,3}$	+7.1	+6.8	+6.8	+5.5	+5.9	7.5	
	4^1H_o,2^1H_p	−1.1	−1.1	−1.1	−1.0	−1.1	0.95	
	4^1H_m	+0.7	+0.6	+0.6	+0.6	+0.6	0.5	
19	$^{14}N_{1,4}$	+6.5	+6.2	+6.1	+4.5	+5.1	5.6	38
	$^{14}N_{2,3}$	+7.1	+6.9	+7.0	+5.7	+6.1	7.5	
20	$^{14}N_{1,3}$	+4.2	+4.1	+3.9	+2.8	+3.2	3.85	39
	$^{14}N_{4,13}$	+5.7	+5.1	+5.2	+3.8	+4.4	7.7	
	$^1H_{5,7,10,12}$	−2.6	−2.7	−2.6	−2.4	−2.5	1.9	
	$^1H_{6,11}$	+0.9	+0.8	+0.7	+0.6	+0.7	0.4	
	$^1H_{8,9}$	+0.5	+0.4	+0.3	+0.3	+0.3	0.4	
21	$^{14}N_{1,2,4,5}$	+5.8	+5.7	+5.5	+4.1	+4.6	6.0	40
	$^1H_3$	+2.3	+2.0	+1.9	+1.7	+1.8	0.72	41
	4^1H_o	−1.4	−1.4	−1.4	−1.2	−1.3	1.10	
	4^1H_m	+0.7	+0.6	+0.6	+0.5	+0.6	0.40	
	2^1H_p	−1.5	−1.5	−1.5	−1.4	−1.5	1.16	
22	$^{14}N_{1,2,4,5}$	+5.7	+5.5	+5.4	+4.0	+4.5	5.9	42
	4^1H_o,2^1H_p	−1.4	−1.5	−1.4	−1.1	−1.4	1.08	41
	4^1H_m	+0.7	+0.6	+0.6	+0.5	+0.6	0.40	
	2^1H_β	−0.1	−0.2	−0.1	−0.1	−0.1	0.08	
	9^1H_γ	+0.1	+0.1	+0.1	+0.1	+0.1	0.11	
23	$^{14}N_{1,2,4,5}$	+5.7	+5.6	+5.4	+4.0	+4.4	5.79	43
	4^1H_o	−1.4	−1.5	−1.4	−1.3	−1.4	1.12	44
	4^1H_m	+0.4	+0.7	+0.6	+0.6	+0.6	0.43	
	2^1H_p	−1.6	−1.6	−1.6	−1.4	−1.5	1.20	
	$2^1H_{o'}$	+0.9	+0.8	+0.8	+0.7	+0.7	0.43	
	$2^1H_{m'}$	−0.4	−0.3	−0.3	−0.3	−0.3	0.16	
	$^1H_{p'}$	+0.7	+0.6	+0.6	+0.5	+0.6	0.31	
	2^1H_β	+0.2	−0.01	+0.02	+0.05	+0.1	0.03	
24	^{14}N	+7.3	+6.8	+7.0	+4.7	+5.6	9.75	45
	$^1H_\alpha$	−11.9	−12.7	−13.0	−12.3	−12.6	12.75	
	2^1H_o,^1H_p	−3.3	−3.2	−3.3	−3.0	−3.2	3.00	
	2^1H_m	+1.5	+1.4	+1.3	+1.2	+1.3	1.00	
25	^{14}N	+7.8	+7.2	+7.3	+5.0	+5.9	10.15	45
	$^1H_\alpha$	−12.2	−12.9	−13.3	−12.5	−12.9	13.75	
	2^1H_o	−3.3	−3.3	−3.3	−3.0	−3.1	3.37	
	2^1H_m	+1.4	+1.3	+1.2	+1.1	+1.2	1.00	
	3^1H_β	+0.4	+0.4	+0.5	+0.4	+0.5	0.50	
26	^{14}N	+6.3	+5.9	+6.0	+3.9	+4.7	7.50	45
	$^{14}N'$	−0.8	−0.6	−0.7	−0.7	−0.7	1.85	
	$^1H_\alpha$	−11.0	−11.7	−12.0	−11.2	−11.6	10.10	
	2^1H_o	−3.1	−3.1	−3.0	−2.8	−2.9	3.00	
	2^1H_m	+1.5	+1.3	+1.3	+1.2	+1.3	0.85	
27	^{14}N	+9.6	+9.1	+9.1	+6.6	+7.5	11.65	46
	$^1H_\alpha$	−13.1	−13.9	−13.9	−13.5	−13.6	12.96	
	2^1H_m	+1.2	+1.1	+1.1	+1.1	+1.1	1.03	
28	^{14}N	+8.9	+7.8	+8.3	+5.8	+6.8	10.65	47
	2^1H_o,^1H_p	−3.1	−3.1	−3.1	−2.8	−3.0	2.75	
	2^1H_m	+1.5	+1.3	+1.2	+1.1	+1.2	1.01	
	3^1H_β	+7.9	+8.4	+8.5	+8.3	+9.0	9.69	
	$^{13}C_\alpha$	−6.0	−5.3	−5.8	−6.2	−6.0	6.0	48
29	^{14}N	+9.8	+8.8	+9.1	+6.7	+7.6	12.08	49
	2^1H_o	−2.9	−2.9	−2.9	−2.6	−2.7	2.09	
	2^1H_m	+1.4	+1.2	+1.2	+1.1	+1.2	0.89	
	^1H_p	−2.9	−2.9	−2.9	−2.7	−2.8	2.29	
	9^1H_γ	+0.03	+0.1	+0.1	+0.1	+0.1	0.09	
30	^{14}N	+8.9	+7.7	+8.3	+5.8	+6.8	11.75	50
	$^1H_{4,6}$	+1.6	+1.4	+1.3	+1.2	+1.3	1.00	
	$^1H_{5,7}$	−3.7	−3.8	−3.7	−3.4	−3.6	3.74	
	2^1H_β	+14.6	+15.0	+15.6	+14.9	+16.5	18.60	
31	^{14}N	+8.4	+7.5	+7.8	+5.5	+6.4	9.66	51
	4^1H_o,2^1H_p	−2.1	−2.1	−2.1	−1.9	−2.0	1.83	
	4^1H_m	+1.2	+1.1	+1.0	+1.0	+1.0	0.79	
32	^{14}N	+6.0	+5.2	+5.6	+3.6	+4.4	6.65	52
	$^1H_{1,3,6,8}$	−2.4	−2.4	−2.4	−2.3	−2.4	2.30	
	$^1H_{2,4,5,7}$	+0.8	+0.8	+0.7	+0.7	+0.7	0.55	
	^{17}O	−17.3	−15.3	−16.4	−10.2	−13.3	16.5	
33	^{14}N	+7.9	+6.8	+7.3	+5.1	+6.0	8.75	52
	$^1H_{1,3,6,8}$	+1.2	+1.1	+1.0	+0.9	+1.0	0.75	
	$^1H_{2,4,5,7}$	−2.6	−2.6	−2.6	−2.4	−2.5	2.30	
	^{17}O	−15.7	−14.9	−14.8	−9.4	−12.0	16.6	
34	^{14}N	+6.3	+5.4	+5.8	+3.9	+4.6	6.89	24
	$^1H_{1,3,6,8}$	+1.1	+1.0	+1.0	+0.9	+0.9	0.69	
	$^1H_{2,7}$	−2.2	−2.2	−2.2	−2.0	−2.1	2.03[c]	
	$^1H_{4,5}$	−2.3	−2.3	−2.3	−2.1	−2.2	2.11[c]	
35	^{14}N	+8.1	+7.0	+7.4	+5.2	+6.1	9.50	52
	$^1H_{1,3,7,9}$	−2.6	−2.7	−2.6	−2.4	−2.6	2.40	
	$^1H_{2,4,6,8}$	+0.9	+0.7	+0.7	+0.6	+0.6	0.50	

Table 1. Continued

no.	nuclei	a_{iso} (theoretical) PBE0/N07D	B3LYP/6-31G*	B3LYP/N07D	B3LYP/TZVP	B3LYP/EPR-III	experimental a_{iso}	ref
36	^{14}N	+8.4	+7.3	+7.7	+5.6	[b]	9.01	53
	$^{1}H_{1,3,7,9}$	−2.4	−2.5	−2.4	−2.2	[b]	2.20	
	$^{1}H_{2,8}$	+1.1	+0.9	+0.9	+0.8	[b]	0.63	
	$^{1}H_{4,6}$	+1.0	+0.8	+0.8	+0.7	[b]	0.50	
37	^{14}N	+8.5	+7.6	+7.8	+5.6	+6.4	10.0	54
	$^{1}H_{\alpha}$	+10.3	+10.9	+10.8	+10.3	+11.2	13.6	
	$2^{1}H_{o}$,$^{1}H_{p}$	−2.5	−2.5	−2.4	−2.2	−2.4	2.5	
	$2^{1}H_{m}$	+1.2	+1.1	+1.0	+0.9	+1.0	0.9	
38	^{14}N	+4.4	+4.5	+4.4	+2.5	+3.2	6.10	55
	$^{1}H_{\alpha}$	−9.4	−10.4	−10.5	−9.9	−10.2	10.40	

[a] All calculations have been carried out on the geometries optimized at B3LYP/6-31G* level of theory. [b] EPR-III basis set is not parametrized for the sulfur nucleus. [c] The assignment of these experimental hfccs has been exchanged taking into account the present theoretical calculations.

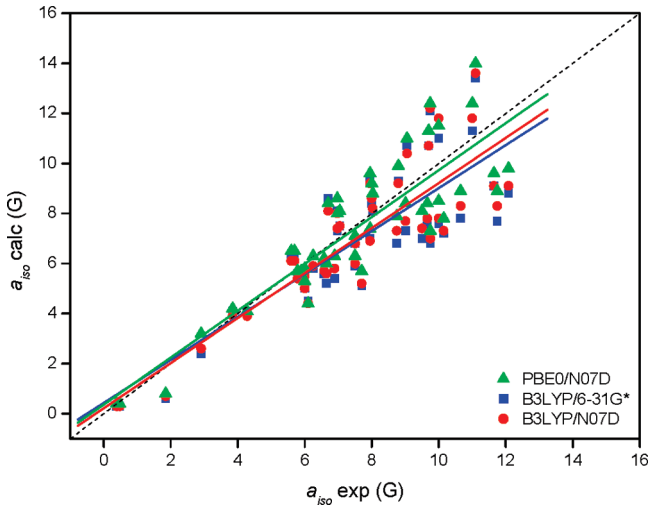

Figure 2. Plot of theoretical vs experimental a_{iso} for ^{14}N nuclei of all studied radicals, calculated at B3LYP/6-31G*, B3LYP/N07D, and PBE0/N07D levels of theory. Linear fits are represented by solid lines.

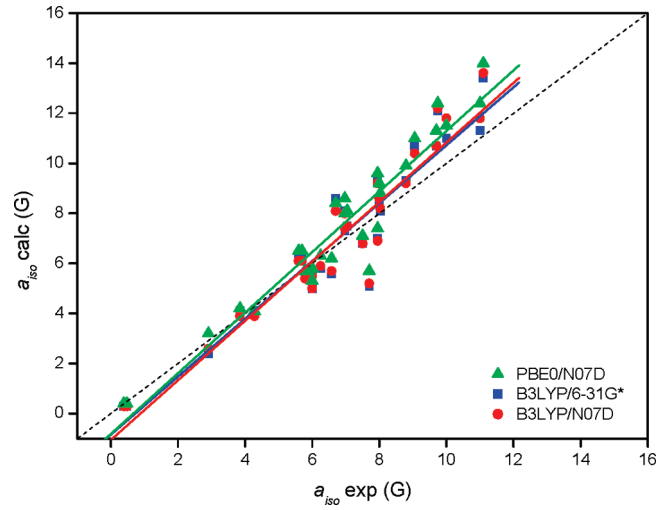

Figure 3. Plot of theoretical vs experimental a_{iso} for ^{14}N nuclei of radicals **1**−**23**, calculated at B3LYP/6-31G*, B3LYP/N07D, and PBE0/N07D levels of theory. Linear fits are represented by solid lines.

basis sets, while 6 *d* functions is mandatory for 6-31G* and N07D basis sets. This result can be clearly observed for a set of ten radicals in Table S2 in the SI, which lists the differences between the a_{iso}(^{14}N) calculated with 5 and 6 *d* functions. From these data, we can conclude that large basis set are not affected by the number of *d* functions (maximum differences of 0.3 G). However, for calculations with medium size basis set, the average differences are around 2G.

In order to get a deeper insight into the results obtained for the nitrogen coupling constants, we have considered in the further analysis only the hfcc data obtained with the N07D and 6-31G* basis sets, because the three combinations, PBE0/N07D, B3LYP/6-31G*, and B3LYP/N07D compute values of ^{14}N hfccs more reliable than those obtained for combinations with EPR-III and TZVP basis sets. However, all the data obtained at the five calculation levels are displayed in Figure S1 in the SI.

Figure 2 represents the calculated vs experimental a_{iso} of ^{14}N for the 38 species, at the three calculation levels above indicated. Although this figure shows an important scattering of the points, interesting conclusions can be achieved if the set of 38 radicals is divided in two subsets, one of them corresponding to the non nitroxide-type radicals, species **1**−**23**, and the other one to the nitroxide-type radicals, species **24**−**38**.

As can be observed in Figures 3 and 4, a_{iso}(^{14}N) of the non nitroxide-type radical subset are predicted quite accurately at the three calculation levels, whereas the ^{14}N hfccs obtained for nitroxide-type radicals are noteworthy underestimated. This result had been previously observed by other authors and analyzed in the terms of the limits of the static gas-phase DFT approaches.[56] In the case of the nitroxide radicals, there are two main critical geometric parameters, namely the improper dihedral angle corresponding to the out-of-plane motion of the NO moiety, and the N−O bond length; a nearly planar environment of nitrogen leads to the lack of any contribution of nitrogen *s* orbitals to the SOMO with the consequent reduction of hfcc. The computation of the magnetic parameter along the trajectory provided by Molecular Dynamics (MD) runs may account for this effect. Indeed, several works[56−60] have shown that the computed a_{iso}(^{14}N) for the planar structures predicted by static models are lower than the values obtained for the averaged ones obtained by molecular dynamic simulations, that are slightly pyramidal. As a matter of fact, all of the nitroxide radicals studied herein are predicted to have optimized geometries

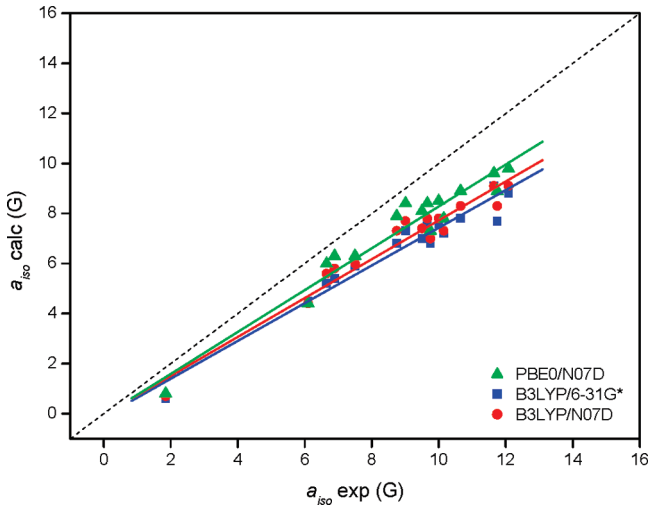

Figure 4. Plot of theoretical vs experimental a_{iso} for ^{14}N nuclei of radicals **24**−**38**, calculated at B3LYP/6-31G*, B3LYP/N07D, and PBE0/N07D levels of theory. Linear fits are represented by solid lines.

with almost planar environment of the nitrogen, which could explain the eventual reduction of the hfcc.

For a better comparison of the general performance and accuracy of the different computational schemes in the prediction of hfccs, a regression analysis was carried out for the five calculation levels included in Table 1. Different parameters of the regression analysis: intercept, slope, correlation coefficient (R^2) of the least-squares fit, as well as the number of data (N), range (minimum and maximum absolute values), absolute error, maximum and mean percent error (E) between calculated and experimental values, mean absolute deviation (MAD), and the ratio range/MAD are collected in Table 2. The analysis was made considering $a_{iso}(^{14}N)$ and the $a_{iso}(^{1}H)$ together and separately, in all the radicals and in the two subsets, non nitroxide and nitroxide-type radicals, as indicate the sections shown in Table 2. The number of data is high enough to infer general conclusions as regards the prediction of this parameter on nitrogen aromatic radicals.

The correlation coefficient (R^2) for the five linear fits considering all the nuclei in the 38 radicals (section *i* in Table 2) is higher than 0.87, being the values of the calculations with B3LYP/TZVP and B3LYP/EPR-III the poorest. The R^2 values for the calculations with the other three levels of theory (N07D and 6-31G* basis sets) are higher (>0.93) and quite similar between each other. The same qualitative tendency is observed when non nitroxide and nitroxide-type radicals are analyzed separately (sections ii and iii in Table 2).

Analyzing the values calculated for $a_{iso}(^{14}N)$, the lowest R^2 value corresponds to the fits where all radical are considered together, $0.65 < R^2 < 0.77$. Correlation coefficient becomes better when both, non nitroxide and nitroxide type radical subsets, are considered separately, arising values higher than 0.9 for almost all fittings (sections v and vi in Table 2).

As expected, for $a_{iso}(^{1}H)$ the correlation coefficient of the five linear fits are very high (>0.96) without significant differences between the two types of radicals, and the best result always corresponds to the B3LYP/EPR-III combination (sections vii−ix in Table 2).

The analysis of the slopes of the least-squares fits also reveals the influence of the basis set and the type of radical, especially in the calculation of the $a_{iso}(^{14}N)$. The value of the slopes in which all nuclei (^{1}H and ^{14}N) have been taken in account are considerably far from the unit for TZVP and EPR-III basis sets, obtaining similar slope values for fittings with N07D and 6-31G* basis sets, and closer to the unit value. According to this parameter, the agreement between theoretical and experimental a_{iso} is much better for non nitroxide-type radicals than for nitroxide-type radicals, since the slopes are much closer to the unity in the former. Especially remarkable is the deviation of the values predicted by the B3LYP/TZVP scheme, which slope for nitroxide-type radicals is ca. 0.70.

Analyzing the values of the ^{14}N hfccs, it is observed that the slopes are scattered from 0.57 to 1.21 (sections v−vi in Table 2) and these values depend strongly on the kind of compounds considered, that is, all radicals together or any of the subsets, nitroxide or non-nitroxide type radicals, separately. So, the values of the slopes for the three lower-cost levels of theory are noticeably higher than the unit for radicals **1**−**23** and smaller than one for radicals **24**−**38**, resulting in slopes closer to the unity when all radicals are analyzed as a whole. However, the bad values of the correlation coefficient for these cases is a signal of the inconsistency of these data, thus, both groups must to be analyzed separately.

The value of the absolute error is not representative of the accuracy of a computational level for the prediction of hfccs since it depends on the range. Nevertheless, comparison of the maximum absolute errors within each subset is coherent. In that regard, we should stress that the values corresponding to the calculations with TZVP and EPR-III basis sets are higher than those with 6-31G* and N07D basis sets, analyzing ^{1}H and ^{14}N together or separately, in the 38 radicals or in the two subsets, non-nitroxide and nitroxide type radicals, except in the analysis of the ^{1}H nucleus, for which notable discrepancies do not become apparent among the five combinations, corresponding lower values of the maximum absolute errors to EPR-III calculations.

The parameter that can be considered as reference for the relative comparison of the accuracy of the different methodologies in the computation of hfccs respect to the corresponding experimental values is the ratio between the range and the mean absolute deviation (range/MAD). The most remarkable result is the lower values of that ratio for the calculations with the two larger basis sets in any subset where ^{14}N hfccs have been included, sections i−vi in Table 2, pointing out that B3LYP/TZVP and B3LYP/EPR-III levels are not suitable for the prediction of $a_{iso}(^{14}N)$ of aromatic radicals in general. However, the opposite result is obtained for the computation of the ^{1}H coupling constant, as the range/MAD values for the combinations with 6-31G* and N07D basis sets are lower. In this case, the ratio for the PBE0/N07D level is the poorest, being the B3LYP/N07D combination the best one of the three less computational demanding

Table 2. Regression Analysis for Predictions of Isotropic Hyperfine Coupling Constants (*G*) of the Studied Radicals

level of theory[a]	intercept	slope	R^2	*N*	$\|a_{iso}\|_{min}$	$\|a_{iso}\|_{max}$	max. absolute error	average *E*%[b]	max *E*%	MAD[c]	range/MAD
(i) all nuclei, all radicals											
PBE0/N07D	0.5389	0.9071	0.9421	161	0.03	14.6	4.0	37	757	0.70	20.93
B3LYP/6-31G*	0.4400	0.8994	0.9306	161	0.01	15.3	4.1	27	186	0.71	21.14
B3LYP/N07D	0.3562	0.9181	0.9417	161	0.02	16.4	3.5	23	186	0.64	24.20
B3LYP/TZVP	0.3468	0.7547	0.8733	161	0.05	14.9	6.0	24	186	0.96	15.41
B3LYP/EPR-III	0.3398	0.8254	0.9120	151	0.1	16.5	5.0	23	233	0.79	20.82
(ii) all nuclei, radicals **1**−**23**											
PBE0/N07D	0.2702	1.0539	0.9838	105	0.1	14.0	2.9	43	757	0.61	22.94
B3LYP/6-31G*	0.1902	1.0429	0.9837	105	0.01	14.7	2.6	30	186	0.55	26.58
B3LYP/N07D	0.1279	1.0451	0.9848	105	0.02	14.5	2.5	25	186	0.51	28.50
B3LYP/TZVP	0.2311	0.8365	0.9577	105	0.05	14.1	3.9	24	186	0.69	20.40
B3LYP/EPR-III	0.2135	0.9099	0.9737	99	0.1	13.8	3.3	25	233	0.55	24.96
(iii) all nuclei, radicals **24**−**38**											
PBE0/N07D	0.5693	0.8029	0.9728	56	0.03	14.6	4.0	27	100	0.87	16.84
B3LYP/6-31G*	0.4369	0.7991	0.9426	56	0.1	15.0	4.1	23	68	1.00	14.87
B3LYP/N07D	0.3719	0.8284	0.9502	56	0.1	15.6	3.5	20	62	0.90	17.26
B3LYP/TZVP	0.2776	0.7010	0.8462	56	0.1	14.9	6.0	23	62	1.48	10.00
B3LYP/EPR-III	0.2743	0.7727	0.8913	52	0.1	16.5	5.0	20	62	1.24	13.20
(iv) ^{14}N nucleus, all radicals											
PBE0/N07D	0.3694	0.9362	0.7700	47	0.4	14.0	2.9	15	57	1.15	11.78
B3LYP/6-31G*	0.4328	0.8581	0.7110	47	0.3	13.4	4.1	18	68	1.32	9.94
B3LYP/N07D	0.2202	0.8997	0.7500	47	0.3	13.6	3.5	17	62	1.24	10.73
B3LYP/TZVP	0.1689	0.6482	0.6580	47	0.4	11.9	6.0	32	62	2.54	4.52
B3LYP/EPR-III	0.2010	0.7323	0.7140	44	0.3	12.4	5.0	24	62	1.91	6.35
(v) ^{14}N nucleus, radicals **1**−**23**											
PBE0/N07D	−0.8090	1.2101	0.9176	31	0.4	14.0	2.9	13	27	0.96	14.19
B3LYP/6-31G*	−0.8441	1.1566	0.9021	31	0.3	13.4	2.6	13	38	0.81	16.11
B3LYP/N07D	−1.0486	1.1880	0.9111	31	0.3	13.6	2.5	13	38	0.84	15.91
B3LYP/TZVP	−0.8054	0.8786	0.8396	31	0.4	11.9	3.9	25	51	1.74	6.63
B3LYP/EPR-III	−0.9376	0.9943	0.8798	29	0.3	12.4	3.3	18	43	1.16	10.44
(vi) ^{14}N nucleus, radicals **24**−**38**											
PBE0/N07D	−0.0806	0.8362	0.9364	16	0.8	9.8	2.9	19	57	1.53	5.87
B3LYP/6-31G*	−0.1105	0.7536	0.9500	16	0.6	9.1	4.1	28	68	2.30	3.70
B3LYP/N07D	−0.0399	0.7767	0.9487	16	0.7	9.1	3.5	24	62	2.02	4.16
B3LYP/TZVP	−0.3337	0.5745	0.9328	16	0.7	6.7	6.0	47	62	4.11	1.46
B3LYP/EPR-III	−0.2609	0.6516	0.9577	15	0.7	7.6	5.0	37	62	3.35	2.06
(vii) ^{1}H nucleus, all radicals											
PBE0/N07D	0.5179	0.8936	0.9683	114	0.03	14.6	4.0	47	757	0.51	28.73
B3LYP/6-31G*	0.4130	0.9538	0.9714	114	0.01	15.0	3.6	31	186	0.46	32.74
B3LYP/N07D	0.3441	0.9613	0.9763	114	0.02	15.6	3.0	26	186	0.40	39.13
B3LYP/TZVP	0.2768	0.9180	0.9771	114	0.05	14.9	3.7	20	186	0.31	47.47
B3LYP/EPR-III	0.2991	0.9533	0.9857	107	0.1	16.5	2.4	23	233	0.33	49.99
(viii) ^{1}H nucleus, radicals **1**−**23**											
PBE0/N07D	0.3940	1.0049	0.9795	74	0.1	14.0	1.6	56	757	0.46	30.33
B3LYP/6-31G*	0.2458	1.0648	0.9862	74	0.01	14.7	1.8	37	186	0.44	33.12
B3LYP/N07D	0.2149	1.0440	0.9876	74	0.02	14.5	1.6	30	186	0.37	39.06
B3LYP/TZVP	0.1607	0.9960	0.9874	74	0.05	14.1	1.2	24	186	0.25	56.14
B3LYP/EPR-III	0.2188	1.0081	0.9898	70	0.1	13.8	1.1	27	233	0.30	46.31
(ix) ^{1}H nucleus, radicals **24**−**38**											
PBE0/N07D	0.6020	0.8315	0.9767	40	0.03	14.6	4.0	30	100	0.60	24.37
B3LYP/6-31G*	0.4654	0.8914	0.9742	40	0.1	15.0	3.6	21	60	0.48	30.75
B3LYP/N07D	0.3935	0.9142	0.9750	40	0.1	15.6	3.0	18	60	0.45	34.52
B3LYP/TZVP	0.3104	0.8743	0.9765	40	0.1	14.9	3.7	13	41	0.43	34.54
B3LYP/EPR-III	0.3212	0.9229	0.9857	37	0.1	16.5	2.4	14	53	0.39	42.17

[a] All calculations have been carried out on the geometries optimized at B3LYP/6-31G* level of theory. [b] E% (percent error) = $|a_{iso}(calc) - a_{iso}(exp)|/a_{iso}(exp)$. [c] MAD(Mean Absolute Deviation) = $1/N\sum_i^N |a_{iso}(calc) - a_{iso}(exp)|$.

methods considered herein. Both the 6-31G* and the N07D basis sets are equally appropriated for the theoretical evaluation of ^{14}N hfccs of aromatic non nitroxide type radicals, but none of the five levels of theory are advisible for such a calculation in nitroxide radicals, given that all the ratios are very low. The thorough comparative analysis of all the parameters in Table 2 enables us to infer that, on balance, the most consistent results are provided by B3LYP/N07D level of theory, since it leads to overall predictions of hfccs of ^{14}N and ^{1}H nuclei of nitrogen aromatic radicals in a reasonable reliability. Unfortunately, the calculation of $a_{iso}(^{14}N)$ in the case of nitroxide radicals is particularly difficult, and all of the tested methodologies considerably underestimate the constants. The lack of reliability of these methods to compute nitrogen hfccs in nitroxide radicals has been previously outlined. A huge quantity of work has been

devoted to the theoretical investigation in depth on these species.[56−70] All of them, with remarkable recognition to the review by Improta and Barone,[56] point out that quantum mechanical methods that perform well for several classes of organic free radicals, do not lead to very good results for nitroxides, especially in the prediction of nitrogen isotropic hyperfine coupling. The disappointing results have been attributed to effects like vibrational averaging, conformational flexibility, and spin delocalization, which could play a significant role in determining this parameter, and are not correctly modeled by a static gas-phase QM approach. The accurate evaluation demands an integrated strategy able to provide a reliable description of the radical electronic structure. The first approach consisted of the correction of the DFT $a_{iso}(^{14}N)$ by means of a term computed with a post-Hartree−Fock method, such as quadratic configuration interaction (QCISD), coupled with purposely tailored basis sets.[56] Several studies have shown that this procedure leads to very good values of the nitrogen hfccs in nitroxides[62−65] but, unfortunately, it is not always applicable because of time-consuming computational difficulties. This is especially the case when both specific and bulk solvent effects, whose inclusion has proven to be non-negligible,[65,68] are properly accounted. More recently, a combination of discrete QM-continuum methods and MD simulations has been proposed as a more feasible integrated strategy, in which the averaged parameters are determined by running a molecular dynamics simulation of the implicit and/or explicit solvated radical and statistically sampling the resulting configurations.[57−60,62−67,69]

The deep analysis of the linear regression parameters calculated herein for ^{14}N nucleus of nitroxide species reveals that good correlations are obtained for the five fits in spite of the low range/MAD ratios. This implies that the theoretical values are far from the experimental ones but the deviation is always systematic, therefore, correctable as now it is known. B3LYP/EPR-III combination has the best correlation coefficient, but the value for the B3LYP/6-31G* fit is almost the same with the advantage of being much less computational demand and applicable to much more atoms than the former. Accordingly, we propose to use the B3LYP/6-31G* level of theory for the calculation of $a_{iso}(^{14}N)$ of nitroxide radicals and to scale the values by means of the linear fit obtained herein for such a calculation, that is:

$$a_N(\text{nitroxide}) = (a_N^{B3LYP/6-31G*} + 0.1105)/0.7536 \quad (1)$$

where both a_N are given in Gauss. Figure 5 shows, as a noteworthy example, the result obtained by application of this equation to the nitroxide radicals studied in this work. The agreement between experimental data of nitrogen hfccs and the scaled-B3LYP/6-31G* values is excellent, with $R^2 > 0.95$, slope ≈ 1, intercept ≈ 0 and range/MAD ≈ 24. Figure S2 in the SI displays the plots resulting from the application of a similar scale procedure to the other four levels of theory. All of them give very satisfactory results, but the range/MAD of the scaled-B3LYP/6-31G* fit is the highest, backing the selection of this computational protocol for this purpose.

Comparison of Figures 4 and 5 clearly indicates the improvement due to the addition of the corrective term

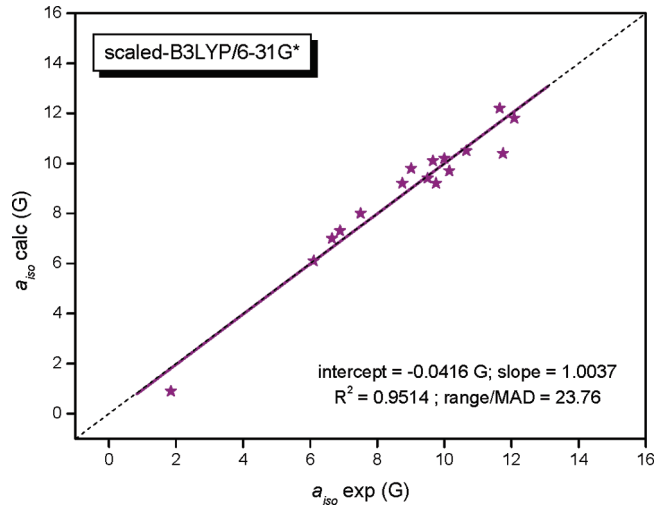

Figure 5. Plot of theoretical vs experimental a_{iso} for ^{14}N nuclei of radicals **24**−**38**, calculated by means of eq (1). The linear fit is represented by a solid line.

provided by the present work, allowing one to obtain reliable values of the ^{14}N hfccs of nitroxide species in a very simple way and with low computational cost.

IV. Conclusions

An extensive study on the calculation of isotropic hyperfine coupling constants of aromatic radicals containing ^{14}N nucleus has been carried out by comparing 165 experimental hfccs to the corresponding data obtained from calculations at five different levels of theory: PBE0/N07D, B3LYP/6-31G*, B3LYP/N07D, B3LYP/TZVP, and B3LYP/EPR-III.

The results indicate that a_{iso} of ^{1}H are predicted in very well agreement with the experimental values regardless of the level of theory employed, whereas significant differences are found in the case of the ^{14}N nucleus, being the selection of the basis set of fundamental importance, specially the number of components of *d* functions. In that regard, 6-31G* and N07D basis sets behave in a similar way in general, and predict hyperfine constants of ^{14}N closer to the experimental values than EPR-III and TZVP basis sets.

The thorough comparison of the results by a regression analysis points out that, on balance, the most consistent results are provided by the B3LYP/N07D level of theory, since it leads to overall predictions of hfccs of ^{14}N and ^{1}H nuclei of nitrogen aromatic radicals in a reasonable reliability.

A different tendency is observed for the calculated $a_{iso}(^{14}N)$ of non nitroxide and nitroxide type radicals. The first group is predicted quite accurately, whereas the values of the second type are considerably underestimated. As is widely known, the calculation of $a_{iso}(^{14}N)$ of nitroxide radicals is of particular complexity, and all the levels of theory investigated herein underestimate them in a great quantity. The N07D basis set combined with the PBE0 functional has shown to provide the most reliable values, albeit still important discrepancies are obtained.

Finally, a simple empirical method to obtain accurate values of the $a_{iso}(^{14}N)$ of nitroxide type radicals is provided, avoiding integrated methodologies which complexity and high computational cost restrict its application. This alterna-

tive consists on properly scaling the values obtained at B3LYP/6-31G* level of theory by means of the data provided by the linear fit corresponding to such a calculation.

Acknowledgment. The "Dirección General de Política Científica" of MEC (Spain) is gratefully acknowledged for financial support (MAT2008-06725-C03-02 and CTQ2010-19232).

Supporting Information Available: The name, the symmetry of the electronic ground state, and the total energies of the minimum of each radical computed at PBE0/N07D, B3LYP/6-31G*, B3LYP/N07D, B3LYP/TZVP, and B3LYP/EPR-III levels of theory (Table S1). Differences between the theoretical isotropic hyperfine coupling constants of ^{14}N nuclei calculated at different levels of theory with 5 and 6 *d* functions, for a subset of ten radicals (Table S2). Plot of theoretical vs experimental a_{iso} for ^{14}N nuclei and ^{1}H nuclei of the studied radicals, calculated at the five different levels of theory (Figure S1). Plot of theoretical vs experimental a_{iso} for ^{14}N nuclei of nitroxide radicals (**24**−**38**), calculated by properly scaling the data obtained at each level of theory (Figure S2). This material is available free of charge via the Internet at http://pubs.acs.org.

References

(1) Likhtenshtein, G. I. Nitroxide Spin Probes for Studies of Molecular Dynamics and Microstructure. In *Nitroxides: Applications in Chemistry, Biomedicine, and Materials Science*; Likhtenshtein, G. I.; Yamauchi, J., Nakatsuji, S., Smirnov, A. I., Tamura, R., Eds.; Wiley-VCH: Weinheim, Germany, 2008; pp 205−238.

(2) Gerson, F.; Huber, W. Electron-Nuclear Magnetic Interaction. In *Electron Spin Resonance Spectroscopy of Organic Radicals*; Wiley-VCH: Weinheim, Germany, 2003; pp 37−48.

(3) Corvaja, C. Introduction to Electron Paramagnetic Resonance. In *Electron Paramagnetic Resonance: A Practitioner'S Toolkit*; Brustolon, M., Giamello, E., Eds.; John Wiley & Sons, Inc.: Hoboken, NJ, 2009; pp 3−36.

(4) Kaupp, M.; Bühl, M.; Malkin, V. G. *Calculation of NMR and EPR Parameters: Theory and Applications*; Wiley-VCH Verlag GmbH & Co. KGaA: Weinheim, 2004. Munzarová, M. L. DFT Calculations of EPR hyperfine Coupling Tensors. In *Calculation of NMR and EPR Parameters: Theory and Applications*; Kaupp, M., Bühl, M., Malkin, V. G., Eds.; Wiley-VCH: Weinheim, Germany, 2004; pp 463−482.

(5) Hermosilla, L.; Calle, P.; de la Vega, J. M. G.; Sieiro, C. *J. Phys. Chem. A* **2005**, *109*, 1114.

(6) Hermosilla, L.; Calle, P.; Sieiro, C. *Phosphorus Sulfur Silicon Relat. Elem.* **2005**, *180*, 1421.

(7) Hermosilla, L.; Calle, P.; de la Vega, J. M. G.; Sieiro, C. *J. Phys. Chem. A* **2005**, *109*, 7626.

(8) Hermosilla, L.; Calle, P.; de la Vega, J. M. G.; Sieiro, C. *J. Phys. Chem. A* **2006**, *110*, 13600.

(9) Becke, A. D. *J. Chem. Phys.* **1993**, *98*, 5648.

(10) Lee, C. T.; Yang, W. T.; Parr, R. G. *Phys. Rev. B* **1988**, *37*, 785.

(11) Godbout, N.; Salahub, D. R.; Andzelm, J.; Wimmer, E. *Can. J. Chem.-Rev. Can. Chim.* **1992**, *70*, 560.

(12) Rega, N.; Cossi, M.; Barone, V. *J. Chem. Phys.* **1996**, *105*, 11060.

(13) Barone, V. *J. Phys. Chem.* **1995**, *99*, 11659.

(14) Hehre, W. J.; Ditchfie, R.; Pople, J. A. *J. Chem. Phys.* **1972**, *56*, 2257.

(15) Harihara, P. C.; Pople, J. A. *Theor. Chim. Acta* **1973**, *28*, 213.

(16) Barone, V.; Cimino, P. *Chem. Phys. Lett.* **2008**, *454*, 139.

(17) Barone, V.; Cimino, P.; Stendardo, E. *J. Chem. Theory Comput.* **2008**, *4*, 751.

(18) Adamo, C.; Barone, V. *J. Chem. Phys.* **1999**, *110*, 6158.

(19) *Gaussian 03, Revision E.01*; Frisch, M. J.; Trucks, G. W.; Schlegel, H. B.; Scuseria, G. E.; Robb, M. A.; Cheeseman, J. R.; Montgomery, J. A., Jr., Vreven, T.; Kudin, K. N.; Burant, J. C.; Millam, J. M.; Iyengar, S. S.; Tomasi, J.; Barone, V.; Mennucci, B.; Cossi, M.; Scalmani, G.; Rega, N.; Petersson, G. A.; Nakatsuji, H.; Hada, M.; Ehara, M.; Toyota, K.; Fukuda, R.; Hasegawa, J.; Ishida, M.; Nakajima, T.; Honda, Y.; Kitao, O.; Nakai, H.; Klene, M.; Li, X.; Knox, J. E.; Hratchian, H. P.; Cross, J. B.; Bakken, V.; Adamo, C.; Jaramillo, J.; Gomperts, R.; Stratmann, R. E.; Yazyev, O.; Austin, A. J.; Cammi, R.; Pomelli, C.; Ochterski, J. W.; Ayala, P. Y.; Morokuma, K.; Voth, G. A.; Salvador, P.; Dannenberg, J. J.; Zakrzewski, V. G.; Dapprich, S.; Daniels, A. D.; Strain, M. C.; Farkas, O.; Malick, D. K.; Rabuck, A. D.; Raghavachari, K.; Foresman, J. B.; Ortiz, J. V.; Cui, Q.; Baboul, A. G.; Clifford, S.; Cioslowski, J.; Stefanov, B. B.; Liu, G.; Liashenko, A.; Piskorz, P.; Komaromi, I.; Martin, R. L.; Fox, D. J.; Keith, T.; Al-Laham, M. A.; Peng, C. Y.; Nanayakkara, A.; Challacombe, M.; Gill, P. M. W.; Johnson, B.; Chen, W.; Wong, M. W.; Gonzalez, C. Pople, J. A. Gaussian, Inc., Wallingford CT, 2004.

(20) Neta, P.; Fessenden, R. W. *J. Phys. Chem.* **1974**, *78*, 523.

(21) Nelsen, S. F.; Landis, R. T.; Kiehle, L. H.; Leung, T. H. *J. Am. Chem. Soc.* **1972**, *94*, 1610.

(22) Preston, K. F.; Sandall, J. P. B.; Sutcliffe, L. H. *Magn. Reson. Chem.* **1988**, *26*, 755.

(23) Mukai, K.; Nishiguchi, H.; Ishizu, K.; Deguchi, Y.; Takaki, H. *Bull. Chem. Soc. Jpn.* **1967**, *40*, 2731.

(24) Neugebauer, F. A.; Bamberger, S. *Chem. Ber.* **1974**, *107*, 2362.

(25) Neugebauer, F. A.; Fischer, H.; Bamberger, S.; Smith, H. O. *Chem. Ber.* **1972**, *105*, 2694.

(26) Scheffler, K.; Stegmann, H. B. *Tetrahedron Lett.* **1968**, *9*, 3619.

(27) Clarke, D.; Gilbert, B. C.; Hanson, P. *J. Chem. Soc., Perkin Trans 2* **1977**, *4*, 517.

(28) Samunl, A.; Neta, P. *J. Phys. Chem.* **1973**, *77*, 1629.

(29) Itoh, M.; Nagakura, S. *Tetrahedron Lett.* **1965**, *6*, 417.

(30) Hermolin, J.; Levin, M.; Ikegami, Y.; Sawayanagi, M.; Kosower, E. M. *J. Am. Chem. Soc.* **1981**, *103*, 4795.

(31) Braun, D.; Peschk, G.; Hechler, E. *Chemiker-Ztg.* **1970**, *94*, 703.

(32) Hyde, J. S.; Robert, C.; Sneed, J.; Rist, G. H. *J. Chem. Phys.* **1969**, *51*, 1404.

(33) Hudson, R. F.; Lawson, A. J.; Record, K. A. F. *J. Chem. Soc., Chem. Commun.* **1974**, *12*, 488.

(34) Dalal, N. S.; Rippmeester, J. A.; Reddoch, A. H. *J. Magn. Reson.* **1978**, *31*, 471.

(35) Biehl, R.; Moebius, K.; O'Connor, S. E.; Walter, R. I.; Zimmermann, H. *J. Phys. Chem.* **1979**, *83*, 3449.

(36) Dalal, N. S.; Kennedy, D. E.; McDowell, C. A. *J. Chem. Phys.* **1974**, *61*, 1689.

(37) Neugebauer, F. A. *Tetrahedron* **1970**, *26*, 4843.

(38) Neugebauer, F. A.; Russell, G. A. *J. Org. Chem.* **1968**, *33*, 2744.

(39) Neugebauer, F. A. *Chem. Ber.* **1969**, *102*, 1339.

(40) Kuhn, R.; Trischmann, H. *Mh. Chem.* **1964**, *95*, 457.

(41) Brunner, H.; Hausser, K. H.; Neugebauer, F. A. *Tetrahedron* **1971**, *27*, 3611.

(42) Neugebauer, F. A. *Tetrahedron* **1970**, *26*, 4853.

(43) Mukai, K.; Yamamoto, T.; Kohno, M.; Azuma, N.; Ishizu, K. *Bull. Chem. Soc. Jpn.* **1974**, *47*, 1797.

(44) Kopf, P.; Morokuma, K.; Kreilick, R. *J. Chem. Phys.* **1971**, *54*, 105.

(45) Barbarella, G.; Rassat, A. *Bull. Soc. Chim. Fr.* **1969**, 2378.

(46) Terabe, S.; Kuruma, K.; Konaka, R. *J. Chem. Soc., Perkin. Trans. 2* **1973**, *9*, 1252.

(47) Nishikawa, T.; Someno, K. *Bull. Chem. Soc. Jpn.* **1974**, *47*, 2881.

(48) Briere, R.; Chapelet-Letourneux, G.; Lemaire, H.; Rassat, A. *Mol. Phys.* **1971**, *20*, 211.

(49) Ishizu, K.; Nagai, H.; Mukai, K.; Kohno, M.; Yamamoto, T. *Chem. Lett.* **1973**, *2*, 1261.

(50) Bruni, P.; Greci, L. *J. Heterocyclic Chem.* **1972**, *9*, 1455.

(51) Fischer, P. H. H.; Neugebauer, F. A. *Z. Naturforsch.* **1964**, *19a*, 1514.

(52) Aurich, H. G.; Hahn, K.; Stork, K.; Weiss, W. *Tetrahedron* **1977**, *33*, 969.

(53) Chiu, M. F.; Gilbert, B. C.; Hanson, P. *J. Chem. Soc. B* **1970**, 1700.

(54) Aurich, H. G.; Hahn, K.; Stork, K. *Angew. Chem.-Int. Ed. Engl.* **1975**, *14*, 551.

(55) Ramsbottom, J. V.; Waters, W. A. *J. Chem. Soc. B* **1966**, 132.

(56) Improta, R.; Barone, V. *Chem. Rev.* **2004**, *104*, 1231.

(57) Pavone, M.; Benzi, C.; De Angelis, F.; Barone, V. *Chem. Phys. Lett.* **2004**, *395*, 120.

(58) Houriez, C.; Ferre, N.; Masella, M.; Siri, D. *J. Chem. Phys.* **2008**, *128*, 244504.

(59) Houriez, C.; Ferre, N.; Masella, M.; Siri, D. *Theochem.-J. Mol. Struct.* **2009**, *898*, 49.

(60) Cimino, P.; Pedone, A.; Stendardo, E.; Barone, V. *Phys. Chem. Chem. Phys.* **2010**, *12*, 3741.

(61) Rajca, A.; Vale, M.; Rajca, S. *J. Am. Chem. Soc.* **2008**, *130*, 9099.

(62) Tedeschi, A. M.; D'Errico, G.; Busi, E.; Basosi, R.; Barone, V. *Phys. Chem. Chem. Phys.* **2002**, *4*, 2180.

(63) Improta, R.; Scalmani, G.; Barone, V. *Chem. Phys. Lett.* **2001**, *336*, 349.

(64) Improta, R.; di Matteo, A.; Barone, V. *Theor. Chem. Acc.* **2000**, *104*, 273.

(65) Saracino, G. A. A.; Tedeschi, A.; D'Errico, G.; Improta, R.; Franco, L.; Ruzzi, M.; Corvaia, C.; Barone, V. *J. Phys. Chem. A* **2002**, *106*, 10700.

(66) Cimino, P.; Pavone, M.; Barone, V. *J. Phys. Chem. A* **2007**, *111*, 8482.

(67) Pavone, M.; Cimino, P.; Crescenzi, O.; Sillanpaa, A.; Barone, V. *J. Phys. Chem. B* **2007**, *111*, 8928.

(68) Owenius, R.; Engstrom, M.; Lindgren, M.; Huber, M. *J. Phys. Chem. A* **2001**, *105*, 10967.

(69) Barone, V. *Chem. Phys. Lett.* **1996**, *262*, 201.

(70) Ikryannikova, L. N.; Ustynyuk, L. Y.; Tikhonov, A. N. *Magn. Reson. Chem.* **2010**, *48*, 337.

CT1006136